Effects of Boundary Conditions on Magnetic Friction

Kentaro Sugimoto

Department of Physics, The University of Tokyo

December 15, 2017

I would like to express my deepest gratitude to Prof. Naomichi Hatano whose enormous support and insightful comments were invaluable during the course of my study. I am also indebt to Ryo Tamura who provided technical help and sincere encouragement. I would also like to express my gratitude to my family for their moral support and warm encouragements.

Abstract

In the present thesis, hogehoge. Moreover, fugafuga.

Contents

Chapter 1

Introduction

The system is one of the simplest model of two-dimensional magnetic friction. Its spatial and spin dimensionality are far from realistic materials around us. However, we can use several facts from the exact solution for the two-dimensional Ising model, which makes the analysis easier than higher-dimensional cases.

Chapter 2

Velocity-driven Non-equilibrium Phase Transitions in Ising Models

Chapter 3

Numerical Simulations

3.1 Setup of the Model

Sliding friction is a form of energy dissipation on the surface between a moving object and its substrate. The dissipated energy is originated in the kinetic energy of the moving object. We here consider constantly moving case in which an external force maintains the motion of the object with endless supply of its kinetic energy. This view leads to its *non-equilibrium steady state*. When the system is in a non-equilibrium steady state, it is often easy to calculate several *energy currents* such as the frictional heat, its power and so on. Applying the view to our case where two square lattices of the Ising model slide against each other, we can formulate the problem as follows.

1. We prepare a square lattice of the Ising model of size $L_x \times L_z$ and impose periodic boundary conditions in the transverse (x) direction. We first set the system in the equilibrium state of a temperature T, whereas we set the open boundary conditions in the longitudinal (z) direction for the moment (fig).

2. We cut the system along the x-direction into two parts, maintaining interactions on the

cut (fig).

3. We slide two parts along the cut plane with relative velocity v. In other words, we shift the upper half by a lattice constant every $1/v$ unit time.

The Hamiltonian of the system is given by

$$\hat{H} = \hat{H}_{\text{upper}} + \hat{H}_{\text{lower}} + \hat{H}_{\text{slip}}(t), \tag{3.1}$$

where

$$\hat{H}_{\text{upper}} := -J \sum_{\langle i,j \rangle \in \text{upper}} \hat{\sigma}_i \hat{\sigma}_j, \tag{3.2}$$

$$\hat{H}_{\text{lower}} := -J \sum_{\langle i,j \rangle \in \text{lower}} \hat{\sigma}_i \hat{\sigma}_j, \tag{3.3}$$

$$\hat{H}_{\text{slip}}(t) := -J \sum_{\langle i,j(t) \rangle \in \text{slip}} \hat{\sigma}_i \hat{\sigma}_{j(t)}, \tag{3.4}$$

where *upper*, *lower* and *slip* represent the set of interacting spin pairs the upper half, the lower half and the slip plane of the entire system. Shift operations lead the system to repeated *pumping* and *dissipation* processes as follows (fig):

1. **Shifting**: A shift operation excites the energy on the slip plane by the ammount $\langle \hat{H}_{\text{slip}}(t') - \hat{H}_{\text{slip}}(t) \rangle_{\text{st}}$. The letter t' denotes the time just after the shift operation from the time t.

2. **Relaxing-1**: The excited energy on the slip plane dispenses to the entire system $\langle \hat{H}_{\text{upper}} + \hat{H}_{\text{lower}} + \hat{H}_{\text{slip}}(t) \rangle_{\text{st}}$.

3. **Relaxing-2**: The excited entire system relaxes toward the equilibrium the heat bath.

We defined the steady state average $\langle \hat{A} \rangle_{\text{st}} := \sum_i A_i p_i^{(\text{st})}$ for an arbitrary observable $\hat{A}$, where $\{A\}_i$ are eigenvalues of $\hat{A}$ and $\{p_i^{(\text{st})}\}$ are steady state probability distribution. Note that the

distribution $\{p_i^{(\mathrm{st})}\}$ are quite different from the equilibrium (canonical) probability distribution $p_i^{(\mathrm{eq})} \propto \exp\left[-E_i/k_{\mathrm{B}}T\right]$. In addition, the distribution $\{p_i^{(\mathrm{st})}\}$ depends on the sliding velocity v, and therefore it has infinite number of families.

The excited and relaxed amounts of energy per unit time correspond to the energy pumping and dissipation, respectively. The energy pumping $P(t)$ and dissipation $D(t)$ are given by

$$P(t) := \sum_{i_v=0}^{v-1} \left\langle \hat{H}_{\mathrm{slip}}\left(t' - 1 + \frac{i_v}{v}\right) - \hat{H}_{\mathrm{slip}}\left(t - 1 + \frac{i_v}{v}\right) \right\rangle_{\mathrm{st}}, \tag{3.5}$$

$$D(t) := \sum_{i_v=0}^{v-1} \left\langle \hat{H}_{\mathrm{slip}}\left(t - 1 + \frac{i_v+1}{v}\right) - \hat{H}_{\mathrm{slip}}\left(t' - 1 + \frac{i_v}{v}\right) \right\rangle_{\mathrm{st}}. \tag{3.6}$$

3.2 Definitions of Physical Quantities

We now consider the case in which that the system is in a non-equilibrium steady state. We define the frictional force density $f(L_z, T)$ by

$$f(L_z, T) := \lim_{L_x \to \infty} \frac{F(L_x, L_z, T)}{L_x}, \tag{3.7}$$

where $F(L_x, L_z, T)$ is the frictional force of a system of size $L_x \times L_z$ at a temperature T. We numerically formulate the large-size limit $L_x \to \infty$ as follows.

Numerical large-size limit $L_x \to \infty$

If the quantity $F(L_x, L_z, T)/L_x$ is independent on L_x, $F(L_x, L_z, T)/L_x$ is a good approximation for $f(L_z, T)$.

In numerical simulations, we calculate the frictional force $F(L_x, L_z, T)$ using its power $D(L_x, L_z, T)$

by the formula

$$F(L_x, L_z, T) = \frac{D(L_x, L_z, T)}{v}, \tag{3.8}$$

where the quantity $D(L_x, L_z, T)$ is the long-time limit of $D(t)$ for the lattice of $L_x \times L_z$ at a temperature T.

We can easily verify the formula (3.8) by considering general cases in which the frictional force and its power are both time dependent. Denoting the frictional force $F(x)$ at the position x, it holds that

$$\int_{t_0}^{t_1} dt\ D(t) = \int_{x(t_0)}^{x(t_1)} dx\ F(x) = \int_{t_0}^{t_1} \frac{dx}{dt} dt\ F(x(t)) = v \int_{t_0}^{t_1} dt\ F(x(t)), \tag{3.9}$$

for a time dependent $D(t)$, because $dx/dt = v$. Under the assumption of a non-equilibrium steady state, in the long-time limit, the integrands in both hand sides of the relation (3.9) are still equal to each other, and hence

$$D(L_x, L_z, T) = vF(L_x, L_z, T). \tag{3.10}$$

From now we call the quantity $D(L_x, L_z, T)$ *energy dissipation*.

Our models always reach non-equilibrium steady states in the long-time limit $t \to \infty$, which depend on the temperature T and the sliding velocity v; We will prove in App. A. We use the fact that $\lim_{t\to\infty} |D(t)| = \lim_{t\to\infty} |P(t)|$ in order to calculate average value $\bar{D}$ with less fluctuation by using the value $\bar{P}$ [1–3]. We therefore have

$$P(L_x, L_z, T) = vF(L_x, L_z, T). \tag{3.11}$$

We also define the bulk energy density $\epsilon_{\rm b}(L_z, T)$ as follows

$$\epsilon_{\rm b}(L_z, T) := \lim_{L_x \to \infty} \frac{E_{\rm b}(L_x, L_z, T)}{L_x L_z}, \tag{3.12}$$

where $E_{\rm b}(L_x, L_z, T)$ is the energy of entire system. Straitforwardly, we define the bulk heat capacity $c_{\rm b}(L_z, T)$ as follows

$$c_{\rm b}(L_z, T) := \frac{\partial \epsilon_{\rm b}(L_z, T)}{\partial T}. \tag{3.13}$$

3.3 Non-equilibrium Monte Carlo Simulation

Energy dissipation process towards the heat bath occurs via a spin flip. This fundamental processes do not only describe equilibrium states, but also non-equilibrium steady states for a fixed temperature T [4]. Using Monte Carlo method, we can simulate this process.

3.3.1 Introduction the Time Scale to Ising Models

The Ising model which we deal with is a kind of kinetic Ising models [4], in which its time dependent statistics plays several important roles. In order to calculate dynamical observables such as the frictional power (3.11) and its dissipation rate (3.8), we have to define *a unit time* for finite size systems. We now consider the case in which a homogeneous spin chain of the volume L and a heat bath with the temperature T are interacting. This system are well described with enough large number of the spins. Denoting such a number N, we can consider two macroscopically equivalent models as follows:

- An N-spin chain with the lattice constant $a = L/N$,

- An $(M \times N)$-spin chain with the lattice constant $a = L/(M \times N)$,

where M is the large number which have the same property as N. Since both of models well describe the system of volume L, typical time scale[1] of each system should be the same. And under the *homogeneousness* assumption that for both models each spin is independently interacting with the heat bath, the dynamics of any spin in the former and that of any M-spins subsystem in the latter are effectively equivalent. Thus as long as we consider the dynamics of same volume systems, we can define the unit time scale using its number of spins. This concept can be easily implemented on the ordinary *equilibrium* Monte Carlo simulation for classical spin systems.

For the equilibrium Monte Carlo simulation, the most naive approach for the equilibrium state is the single flip algorithm, where we perform the sequence a random selection of the spin and its flipping with temperature dependent probability $p(T)$. We often use the Metropolis probability $p_{\mathrm{M}}(T) := \min\{1, \mathrm{e}^{-\frac{\Delta E}{k_{\mathrm{B}}T}}\}$ as the probability $p(T)$, where ΔE is the energy difference by the flipping. The Metropolis probability $p_{\mathrm{M}}(T)$ have a good property, called *detailed balanced condition*, which certainly leads the system towards the true equilibrium state with enough many repetition of the algorithm. This process and randomness well describes the interaction and the homogeneousness with the heat bath. We often call *Monte Carlo step* a single process of the algorithm, and define *Monte Carlo sweep* N-times process, where N is the number of spins. According to the earlier discussion, the unit time in the system is nothing but the Monte Carlo sweep. Thus the more spins the system contains, the higher time resolution we can simulate with.

[1] If we use the same criterion, any time scale may be introduced. For example, we can define *a typical time scale* as the time taken to flip all the spin.

3.3.2 Slip Plane with the Velocity v

Using the introduced time scale, we can also introduce the slip plane with the velocity v to the system with N-spins. Corresponding to the setup in Sec. 3.1, we perform the extended single flip algorithm as follows:

1. **Shifting**: We shift the upper half by a lattice constant.

2. **Flipping**: We perform ordinary single flips for N/v times.

3. We repeat the process 1 + 2 for $(v-1)$ times.

In the extended algorithm, the upper half slides with the velocity v in a unit time at regular intervals. We proved the fact that this algorithm lead the system of any size to the non-equilibrium steady state depending the temperature T and the velocity v (see appA in detail).

3.3.3 Calculation Method

The observables which we are interested in are the frictional power $P(t)$ and its dissipation rate $D(t)$. In Monte Carlo simulations, the frictional power $P(t)$ and the dissipation rate $D(t)$ are the energy difference by the shifting operation and that by the flipping respectively, for a unit time. Both observables have the same absolute value in the long time limit.

Chapter 4

Result of Simulation

4.1 Settings of the Parameters

In the simulation, we fixed the velocity to $v = 10$ and the parameter regions for the temperatures T and the longitudinal size L_z are set as follows:

$$\frac{k_{\rm B}T}{J} \in \{0.0, 0.1, 0.2, \ldots, 1.9, 2.0, 2.02, 2.04, \ldots, 2.48, 2.50, 2.6, 2.7, \ldots, 5.0\}, \tag{4.1}$$

$$L_z \in \{4, 6, 8, 10, 12, 14, 16\}. \tag{4.2}$$

For all the parameters, we relaxed the system for 5000 [MCs] toward the equilibrium state and relaxed for 5000 [MCs] toward the non-equilibrium stead, y state by switching to nonzero v, using Metropolis probability $p_{\rm M}(T)$.

The quantities which we show are the frictional force density $f(L_z, T)$ and the bulk energy density $\epsilon_{\rm b}(L_z, T)$ for two cases that the boundary conditions on the z-direction are *anti-parallel* and *parallel*. For all the quantities, we performed *sample average* over 480 samples and *time average* over the latter 4500 [MCs][1]. We also show the temperature derivative for these quan-

[1]This time length for averaging is based on the criterion that it is much longer than the correlation time of

tities.

The convergence of $F(L_x, L_z, T)/L_x$ and $E_{\rm b}(L_x, L_z, T)/L_x L_z$ in the limit $L_x \to \infty$ was checked (see appB.1 in detail).

4.2 Behavior of Frictional Force Density $f(L_z, T)$

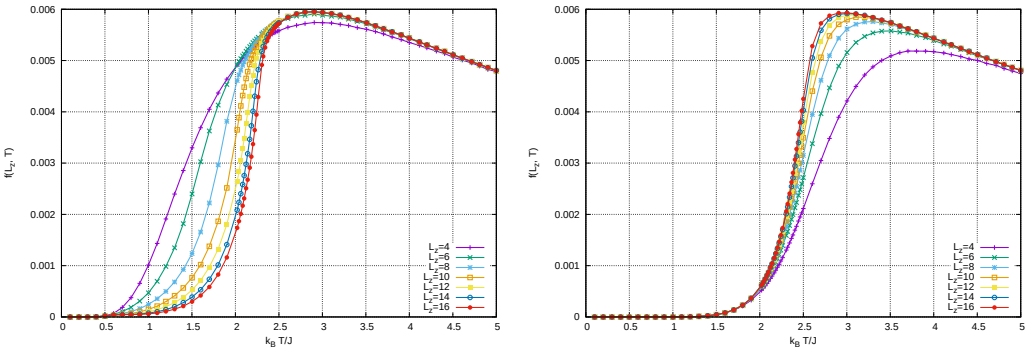

(a) Anti-parallel boundary condition (b) Parallel boundary condition

Figure 4.1: The temperature T dependence of the frictional force density $f(L_z, T)$ with the parallel boundary condition along the z-direction for each longitudinal size L_z are plotted.

4.3 Behavior of Bulk Energy Density $\epsilon_{\rm b}(L_z, T)$

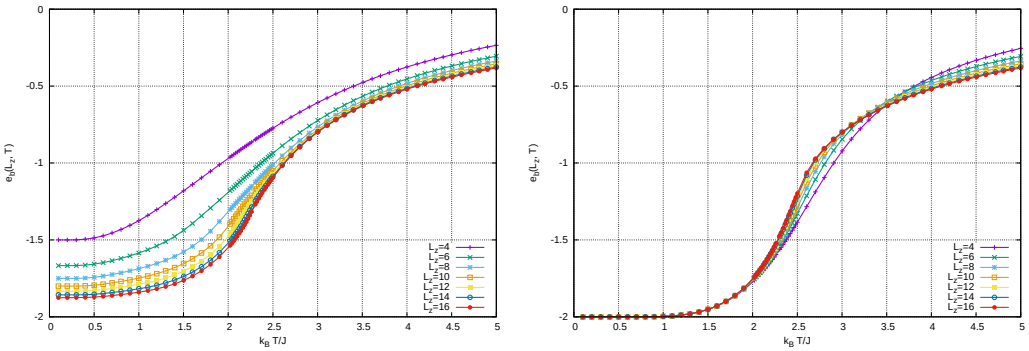

(a) Anti-parallel boundary condition (b) Parallel boundary condition

Figure 4.2: The temperature T dependence of the bulk energy density $\epsilon(L_z, T)$ with the parallel boundary condition along the z-direction for each longitudinal size L_z are plotted.

the system, and the former data over $5000 + 500$ [MCs] are unwanted. The correlation time for each parameter is estimated by checking the relaxation of $P(t)$ and $D(t)$.

4.4 Behavior of Bulk Heat Capacity $c_{\mathrm{b}}(L_z, T)$

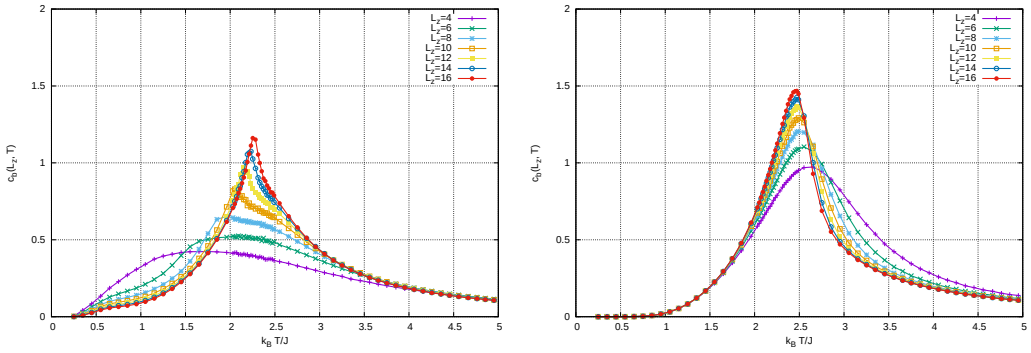

(a) Anti-parallel boundary condition (b) Parallel boundary condition

Figure 4.3: The temperature T dependence of the bulk heat capacity $c(L_z, T)$ with the anti-parallel/parallel boundary condition along the z-direction for each longitudinal size L_z are plotted.

Chapter 5

Summary and Discussion

Summary.

Appendix A

Proof of the existence of NESS

A.1 Stochastic Matrices for Ordinary Monte Carlo Simulations

A.1.1 The Relation between Monte Carlo Simulations and Stochastic Matrices

Monte Carlo simulation extracts the relevant subspace from the true state space instead of calculating the partition function of the system, using the stochastic process. The subspace depends on the temperature, where we can approximately calculate observables.

We now consider a matrix form of the stochastic process. For example, one-dimensional Ising chain with N-spins has 2^N states, thus we can label each state by $i = 1, 2, \ldots, 2^N$. Under the assumption of stochastic time evolution, we can also define the probability $p_i(t)$ that the system is in the i-th state at a time t.

Furthermore, we denote the conditional probability $\tilde{p}_{ij}(t)$ that the system is in the j-th state at a time t and in the i-th state at the next time $t+1$, we can define the transition probability

M_{ij} from the i-th state to the j-th state by

$$\tilde{p}_{ij}(t+1) = M_{ij} p_j(t) \quad \text{for } 1 \leq i, j \leq 2^N. \tag{A.1}$$

From the property of $p_i(t)$ as the probability, it should hold that $\sum_{i=1}^{2^N} p_i(t) = 1$ and $p_i(t) \geq 0$ $(i = 1, 2, \ldots, 2^N)$. In addition, summation $\tilde{p}_{ij}(t)$ over all previous states $j = 1, 2, \ldots, 2^N$ is nothing but $p_i(t+1)$:

$$p_i(t+1) = \sum_{j=1}^{2^N} \tilde{p}_{ij}(t+1) = \sum_{j=1}^{2^N} M_{ij} p_j(t) \quad \text{for } 1 \leq i \leq 2^N. \tag{A.2}$$

Therefore the system can be described by the stochastic time evolution of the probability vector $\boldsymbol{p}(t) := {}^{\mathrm{t}}(p_1(t), p_2(t), \ldots, p_{2^N}(t))$ by the stochastic matrix $\hat{M} := (M_{ij})$:

$$\boldsymbol{p}(t+1) = \hat{M} \boldsymbol{p}(t). \tag{A.3}$$

The normalization property of $\{p_i(t)\}$ is expressed as the L^1-norm property of $\boldsymbol{p}(t)$:

$$\|\boldsymbol{p}(t)\|_1 = 1, \tag{A.4}$$

where the L^1-norm is defined for any vector $\boldsymbol{x} = {}^{\mathrm{t}}(x_1, x_2, \ldots, x_{2^N})$ by $\|\boldsymbol{x}\| := \sum_{i=1}^{2^N} x_i$. And it leads that

$$\sum_{i=1}^{2^N} p_i(t+1) = \sum_{i=1}^{2^N} \sum_{j=1}^{2^N} M_{ij} p_j(t) = \sum_{j=1}^{2^N} \left(\sum_{i=1}^{2^N} M_{ij} \right) p_j(t), \tag{A.5}$$

$$\overset{\|\boldsymbol{p}(\bullet)\|_1 = 1.}{\Longleftrightarrow} \sum_{i=1}^{2^N} M_{ij} = 1 \quad \text{for } 1 \leq i \leq 2^N. \tag{A.6}$$

In addition, we impose the non-negative condition on M_{ij} as the transition probability:

$$M_{ij} \geq 0 \quad \text{for } 1 \leq i, j \leq 2^N. \tag{A.7}$$

Any matrix with conditions (A.6) and (A.7) is called *stochastic matrix* and shows following interesting properties:

- All absolute values of eigenvalue are less than or equal to 1.
- For any eigenvector $\boldsymbol{x} = {}^{\mathrm{t}}\{x_1, x_2, \ldots, x_{2^N}\}$ which does *not* belong to 1, it holds that

$$\sum_{i=1}^{2^N} x_j = 0. \tag{A.8}$$

Furthermore, if we use the Metropolis probability $p_{\mathrm{M}}(t)$ the stochastic matrix $\hat{M}$ which corresponds to a Monte Carlo step satisfies following property so called *strong connectivity*:

$$\left(\hat{M}^{N_0}\right)_{ij} > 0 \quad \text{for arbitrary } (i, j) \text{ at a } N_0 > 0. \tag{A.9}$$

A.1.2 Desired Conditions for Stochastic Matrices and their Results

If the stochastic matrix for our considered Monte Carlo simulation satisfies the strong connectivity, we can maintain that the simulation certainly converges to the equilibrium state from the properties of corresponding stochastic matrix.

We first define the column vector $\boldsymbol{d} := {}^{\mathrm{t}}(1, 1, \ldots, 1)$. For any stochastic matrix $\hat{T}$, we have

$$\left({}^{\mathrm{t}}\hat{T}\boldsymbol{d}\right)_i = \sum_{j=1}^{N} \left({}^{t}T\right)_{ij} d_j = \sum_{j=1}^{N} T_{ji} d_j = \sum_{j=1}^{N} T_{ji} = 1 \quad \text{for } i = 1, 2, \ldots, N, \tag{A.10}$$

$$\iff \quad {}^{\mathrm{t}}\hat{T}\boldsymbol{d} = \boldsymbol{d}. \tag{A.11}$$

Therefore the matrix ${}^{\mathrm{t}}\hat{T}$ has an eigenvalue 1 at least. The eigenequation for the matrix ${}^{\mathrm{t}}\hat{T}$ are rewritten as

$$\det\left[\lambda\hat{I}_N - {}^{\mathrm{t}}\hat{T}\right] = \det\left[{}^{\mathrm{t}}\left(\lambda\hat{I}_N - \hat{T}\right)\right] = \det\left[\lambda\hat{I}_N - \hat{T}\right], \tag{A.12}$$

and then the set of eigenvalues of $\hat{T}$ is equal to that of ${}^{\mathrm{t}}\hat{T}$. Finally the matrix $\hat{T}$ has an eigenvalue 1 at least.

A general eigenvalue equation of $\hat{T}$ can be written as

$$\hat{T}\boldsymbol{x}_\lambda = \lambda\boldsymbol{x}_\lambda, \tag{A.13}$$

where $\boldsymbol{x}_\lambda = {}^{\mathrm{t}}(x_{\lambda,1}, x_{\lambda,2}, \ldots, x_{\lambda,N})$ is its eigenvector. We have

$$((l.h.s \text{ of A.13}), \boldsymbol{d}) = (\hat{T}\boldsymbol{x}_\lambda, \boldsymbol{d}) = (\boldsymbol{x}_\lambda, {}^{\mathrm{t}}\hat{T}\boldsymbol{d}) = (\boldsymbol{x}_\lambda, \boldsymbol{d}), \tag{A.14}$$

$$((r.h.s \text{ of A.13}), \boldsymbol{d}) = (\lambda\boldsymbol{x}_\lambda, \boldsymbol{d}) = \lambda(\boldsymbol{x}_\lambda, \boldsymbol{d}). \tag{A.15}$$

$$\Longleftrightarrow \quad (1-\lambda)(\boldsymbol{x}_\lambda, \boldsymbol{d}) = 0 \quad \Longleftrightarrow \quad \lambda = 1 \text{ or } (\boldsymbol{x}_\lambda, \boldsymbol{d}) = 0. \tag{A.16}$$

$$\Longleftrightarrow \quad \sum_{i=1}^{N} x_{\lambda,i} = 0 \quad \text{if } \lambda \neq 1. \tag{A.17}$$

We additionally define the vector $\boldsymbol{y}_\lambda := {}^{\mathrm{t}}(|x_{\lambda,1}|, |x_{\lambda,2}|, \ldots, |x_{\lambda,N}|)$ for any λ. From the equation $\sum_{j=1}^{N} T_{ij}x_{\lambda,j} = \lambda x_i (i = 1, 2, \ldots, N)$ we have

$$|\sum_{j=1}^{N} T_{ij}x_{\lambda,j}| \leq \sum_{j=1}^{N} T_{ij}|x_{\lambda,j}| \quad (\because T_{ij} \geq 0 \quad \text{for } j = 1, 2, \ldots, N) \tag{A.18}$$

$$= \left(\hat{T}\boldsymbol{y}_\lambda\right)_i \quad \text{for } i = 1, 2, \ldots, N. \tag{A.19}$$

and the left hand side of (A.19) are rewritten as

$$|\sum_{j=1}^{N} T_{ij} x_{\lambda,j}| = |\lambda x_{\lambda,j}| = |\lambda| \times |x_{\lambda,j}| = |\lambda| \times (\boldsymbol{y}_\lambda)_j \,, \tag{A.20}$$

thus we have

$$|\lambda| \times (\boldsymbol{y}_\lambda)_j \leq \left(\hat{T}\boldsymbol{y}_\lambda\right)_i \,, \tag{A.21}$$

$$\iff \quad |\lambda| \times (\boldsymbol{y}_\lambda, \boldsymbol{d}) \leq \left(\hat{T}\boldsymbol{y}_\lambda, \boldsymbol{d}\right) = \left(\boldsymbol{y}_\lambda, {}^{\mathrm{t}}\hat{T}\boldsymbol{d}\right) = (\boldsymbol{y}_\lambda, \boldsymbol{d}) \,, \tag{A.22}$$

$$\iff \quad |\lambda| \leq 1. \tag{A.23}$$

Weak Connectivity of the Matrix $\hat{T}$

For an arbitrary $1 \leq i, j \leq N$, if there exists an $n(i,j) > 0$ such that

$$\left(\hat{T}^{n(i,j)}\right)_{ij} > 0, \tag{A.24}$$

the matrix $\hat{T}$ is called *weakly connected*. Note that for any $n' > n(i,j)$ it does *not* follows that $\left(\hat{T}^{n'}\right) > 0$.

We denote the maximum value of $n(i,j)$ by $n_{\max} := \max_{1 \leq i,j \leq N} [n(i,j)]$ and define the matrix $\hat{\mathcal{T}}_\epsilon := \left(\hat{I}_N + \epsilon\hat{T}\right)^{n_{\max}}$ $(\epsilon > 0)$. We have

$$\left(\hat{\mathcal{T}}_\epsilon\right)_{ij} = \left(\left(\hat{I}_N + \epsilon\hat{T}\right)^{n_{\max}}\right)_{ij} = \sum_{k=1}^{n_{\max}} \binom{n_{\max}}{k} \left(\hat{I}_N^k \left(\epsilon\hat{T}\right)^{n_{\max}-k}\right)_{ij} \tag{A.25}$$

$$= \sum_{k=1}^{n_{\max}} \binom{n_{\max}}{k} \epsilon^{n_{\max}-k} \left(\hat{T}^{n_{\max}-k}\right)_{ij} \geq 0 \quad (\because T_{ij} > 0) \quad \text{for } 1 \leq i, j \leq N. \tag{A.26}$$

For the eigenvector $\boldsymbol{x}_1 = {}^{\mathrm{t}}(x_{1,1}, x_{1,2}, \ldots, x_{1,N})$, which belongs to the eigenvalue 1, it holds

that

$$\hat{\mathcal{T}}_\epsilon \boldsymbol{x}_1 = \sum_{k=1}^{n_{\max}} \binom{k}{n_{\max}} \epsilon^{n_{\max}-k} \hat{T}^{n_{\max}} \boldsymbol{x}_1 \tag{A.27}$$

$$= \sum_{k=1}^{n_{\max}} \binom{k}{n_{\max}} \epsilon^{n_{\max}-k} \boldsymbol{x}_1 \tag{A.28}$$

$$= (1+\epsilon)^{n_{\max}} \boldsymbol{x}_1, \tag{A.29}$$

and each component is

$$\sum_{j=1}^{N} \left(\hat{\mathcal{T}}_\epsilon\right)_{ij} x_{1,j} = (1+\epsilon)^{n_{\max}} x_{1,i} \quad \text{for } i = 1, 2, \ldots, N. \tag{A.30}$$

Now we prove that phases of each component for the vector $\boldsymbol{x}_1$ are aligned together and all the components are positive. In other words, we can decompose the vector into a phase factor and a positive vector as follows

$$\boldsymbol{x}_1 = \mathrm{e}^{i\theta} \boldsymbol{u}_1, \tag{A.31}$$

where all components of $\boldsymbol{u}_1$ are positive.

If components of the vector $\boldsymbol{x}_1$ are *not* aligned together such that $\sum_{i=1}^{N} |x_{1,i}| > |\sum_{i=1}^{N} x_{1,i}|$ holds, we have

$$|\sum_{j=1}^{N} \hat{\mathcal{T}}_{ij} x_{1,j}| < \sum_{j=1}^{N} \hat{\mathcal{T}}_{ij} |x_{1,j}| = (1+\epsilon)^{n_{\max}} |x_{1,i}|. \tag{A.32}$$

On the other hand, the row-wise sum of the matrix $\hat{\mathcal{T}}_\epsilon$ are

$$\sum_{i=1}^{N}\left(\hat{\mathcal{T}}_\epsilon\right)_{ij} = \sum_{k=1}^{n_{\max}}\binom{k}{n_{\max}}\epsilon^{n_{\max}-k}\sum_{i=1}^{N}\left(\hat{T}^{n_{\max}-k}\right)_{ij} = (1+\epsilon)^{n_{\max}}. \tag{A.33}$$

Then we have

$$\sum_{i=1}^{N}\sum_{j=1}^{N}\hat{\mathcal{T}}_{ij}|x_{1,j}| = (1+\epsilon)^{n_{\max}}\sum_{j=1}^{N}|x_{1,j}| > (1+\epsilon)^{n_{\max}}\sum_{i=1}^{N}|x_{1,i}|, \tag{A.34}$$

but it is the contradiction caused from our assumption $\sum_{i=1}^{N}|x_{1,i}| > |\sum_{i=1}^{N}x_{1,i}|$. Furthermore the left hand side of (A.30) is positive because that $n_{\max}$ is the maximum value of $n(i,j)$ which the element $\left(\hat{\mathcal{T}}_{ij}^{n(i,j)}\right) > 0$, and then the right hand side is also positive. Then we have $x_{1,i} > 0 (i = 1, 2, \ldots, N)$.

Next we prove that the eigenspace of the matrix $\hat{\mathcal{T}}_{ij}$, which belongs to the eigenvalue 1 is *one-dimensional*. If we have two different eigenvectors, which belongs to the eigenvalue 1, we can write their eigenequations by two different *positive vectors* as

$$\hat{T}\boldsymbol{u}_1 = u_1, \tag{A.35}$$

$$\hat{T}\boldsymbol{v}_1 = v_1. \tag{A.36}$$

For their any linear superposition, we also have

$$\hat{T}(\boldsymbol{u}_1 + t v_1) = \boldsymbol{u}_1 + t v_1 \quad \text{for any } t \in \mathbb{R}. \tag{A.37}$$

If two eigenvectors $\boldsymbol{u}_1$ and $\boldsymbol{v}_1$ are not aligned, we can make a non-trivial vector with a certain t such that $(\boldsymbol{u}_1 + t v_1)_l = 0$ for an l-th element. But it is the contradiction with the fact

$x_{1,i} > 0 (i = 1, 2, \ldots, N)$. Then we have no eigenspaces more than one, which belongs the eigenvalue 1.

In the end of this subsection, we will prove the existence of the limit $\lim_{N\to\infty} \hat{T}^N \boldsymbol{p}^{(0)}$ and its uniqueness with the condition called *strong connectivity* of the matrix $\hat{T}^N$. This condition is summarized as follows.

Strong Connectivity of the Matrix $\hat{T}$

If there exists a number $N_0 > 0$ such that

$$\left(\hat{T}^{N_0}\right)_{ij} > 0 \tag{A.38}$$

for an arbitrary $1 \leq i, j \leq N$, the matrix $\hat{T}$ is called *strongly connected*.

The stochastic matrix which corresponds to a Monte Carlo simulation is often strongly connected, and hence we can ensure the uniqueness of long time limit for our Monte Carlo simulation.

We first prove that there exists only the eigenvalue 1 with its absolute value 1. And then prove that $\lim_{N\to\infty} \hat{T}^N \boldsymbol{r} = \boldsymbol{0}$ for any $\boldsymbol{r} \in \mathbb{C}$ orthogonal to $\boldsymbol{d}$, and we can write any *initial* vector $\boldsymbol{p}^{(0)}$ as the superposition of $\boldsymbol{u}_1$ and $\boldsymbol{r}$. These two facts lead to the relation $\lim_{N\to\infty} \hat{T}^N \boldsymbol{p}^{(0)} = \boldsymbol{u}_1 / \|\boldsymbol{u}_1\|_1$.

A.1.3 Construction the Stochastic Matrix for Simple Systems

Cite the mathematica results.

A.2 Stochastic Matrices for Non-Equilbrium Monte Carlo Simulations

A.3 Calculation Non-Equilbrium Observables by the Stochastic Matrices

Appendix B

Results of Simulations in More Detail

B.1 Checking the Convergence in the Limit $L_x \to \infty$

We now demonstrate that following two observables are converging at corresponding numerical large size limits.

$$f(L_z, T) := \lim_{L_x \to \infty} \frac{F(L_x, L_z, T)}{L_x} \tag{B.1}$$

$$\epsilon_{\mathrm{b}}(L_z, T) := \lim_{L_x \to \infty} \frac{E_b(L_x, L_z, T)}{L_x L_z} \tag{B.2}$$

Both of them have no dependence on L_x and also do not diverge in the limit of L_z. Thus we can analyze these qualitative and pure dependence on L_z and T. We use the aspect of $L_x = 10L_z, 20L_z, \ldots, 50L_z$ for checking the convergence in the limit $L_x/L_z \to \infty$ with fixed L_z.

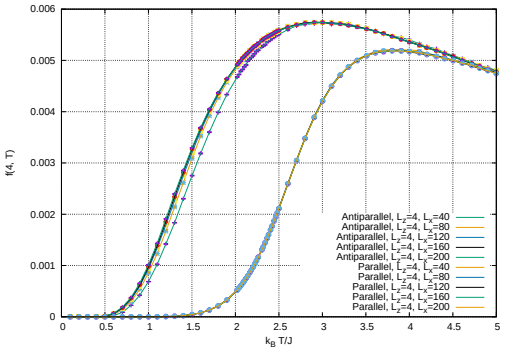

(a) $L_z = 4$

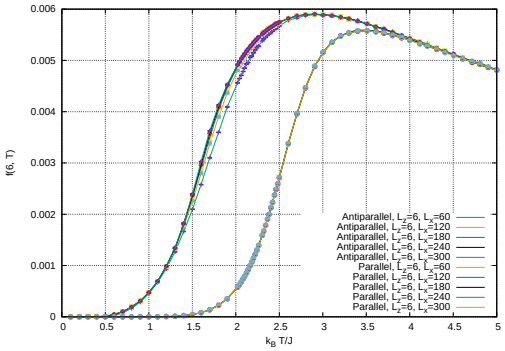

(b) $L_z = 6$

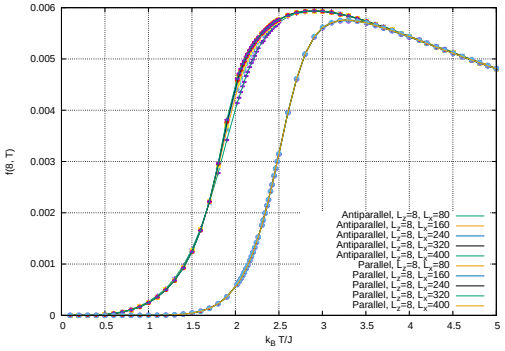

(c) $L_z = 8$

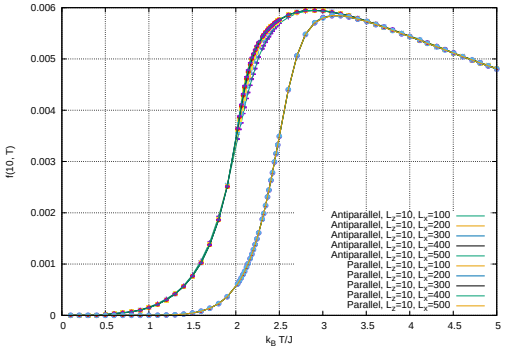

(d) $L_z = 10$

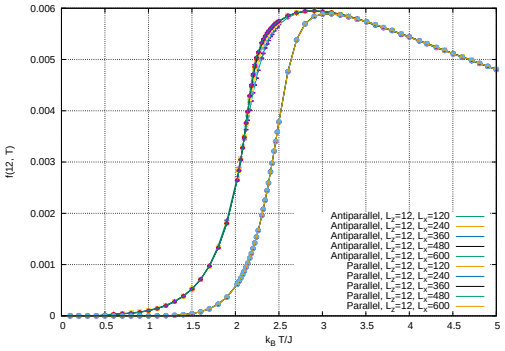

(e) $L_z = 12$

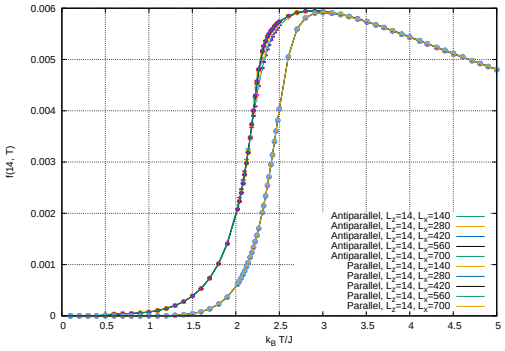

(f) $L_z = 14$

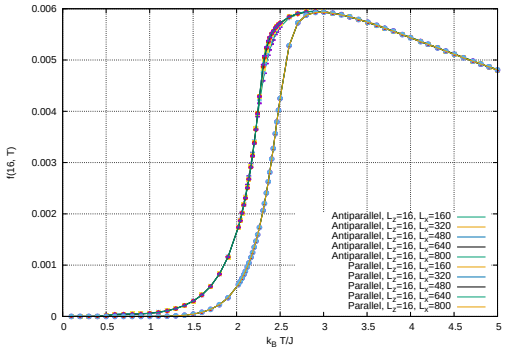

(g) $L_z = 16$

Figure B.1: Each data shows $F(L_x, L_z, T)/L_x$ versus T.

B.1.1 Dependence of $F(L_x, L_z, T)/L_x$ on L_x for each L_z

We show that the quantity $F(L_x, L_z, T)/L_x$ has no dependence on L_x at a sufficient large L_x for each L_z. The following graphs are the temperature dependence of the frictional force density with each of boundary conditions along the z-direction for each of longitudinal size $L_z = 4, 6, 8, 10, 12, 14, 16$ (fig.B.1).

B.1.2 Dependence of $E_{\rm b}(L_x, L_z, T)/(L_x L_z)$ on L_x for each L_z

We show that the quantity $E_{\rm b}(L_x, L_z, T)/L_x$ has no dependence on L_x at a sufficient large L_x for each L_z. The following graphs are the temperature dependence of the frictional force density with each of boundary conditions along the z-direction for each of longitudinal size $L_z = 4, 6, 8, 10, 12, 14, 16$ (fig.B.2).

B.2 Time Series of Observables

We now show the data which we use to calculate the long time limit of power $P(t)$, dissipation rate $D(t)$ and bulk energy $E_{\rm b}(t)$.

We can estimate the non-equilibrium correlation time of these observables, and then the valid interval in each time series are determined.

B.2.1 title

title

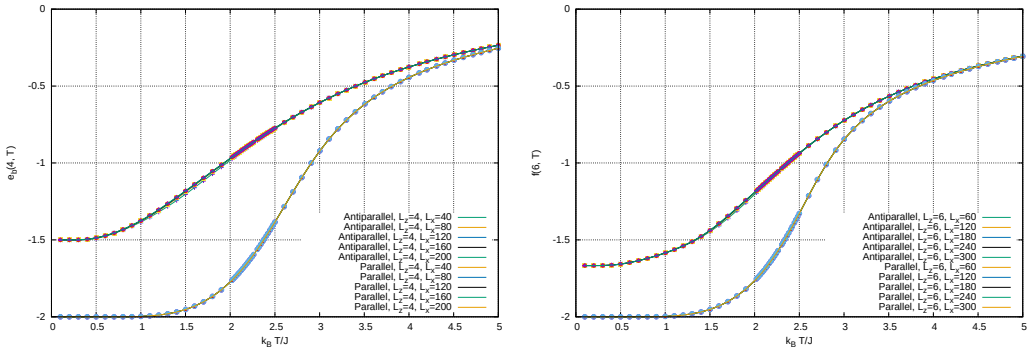

(a) $L_z = 4$

(b) $L_z = 6$

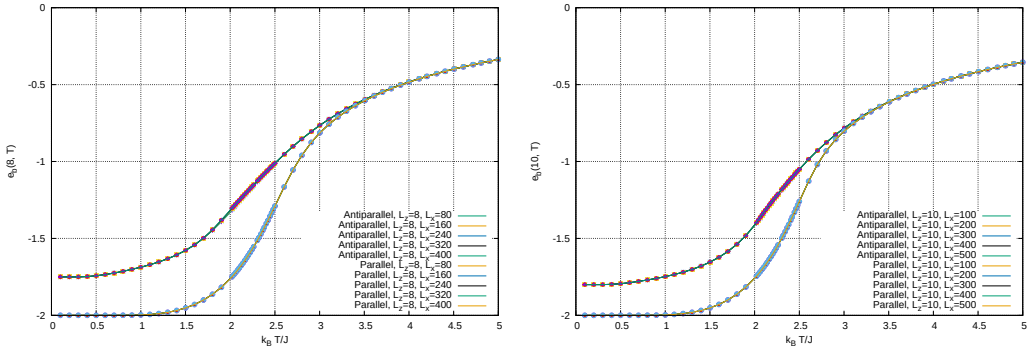

(c) $L_z = 8$

(d) $L_z = 10$

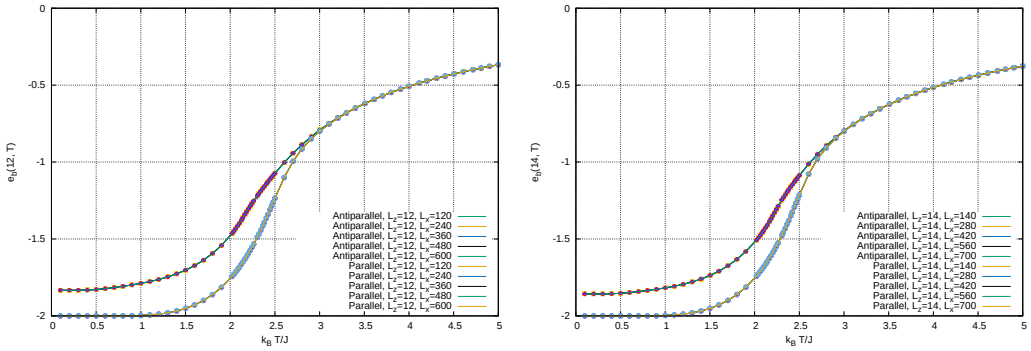

(e) $L_z = 12$

(f) $L_z = 14$

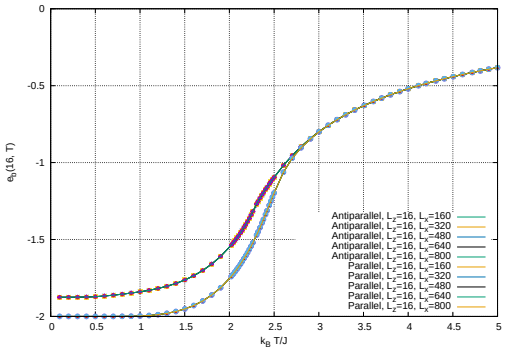

(g) $L_z = 16$

Figure B.2: Each data shows $E(L_x, L_z, T)/(L_x L_z)$ versus T.

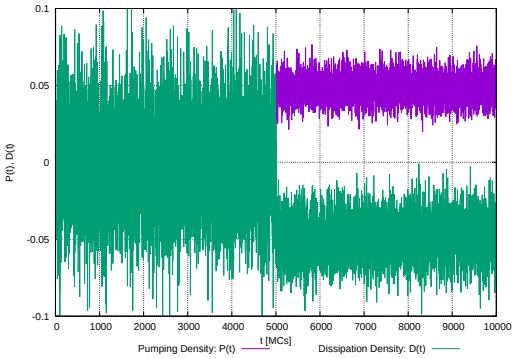
0.1
0.05
0
-0.05
-0.1
P(t), D(t)
0
1000
2000
3000
4000
5000
6000
7000
8000
9000
10000
t [MCs]
Pumping Density: P(t)
Dissipation Density: D(t)

(a) $T = 5.0$

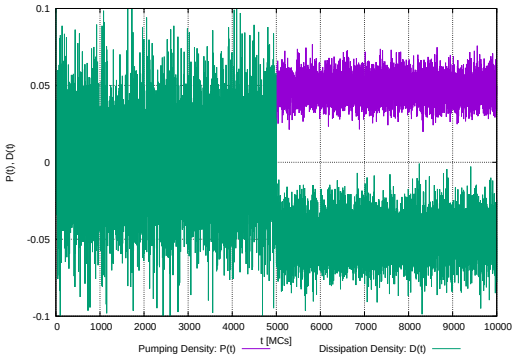
0.1
0.05
0
-0.05
-0.1
P(t), D(t)
0
1000
2000
3000
4000
5000
6000
7000
8000
9000
10000
t [MCs]
Pumping Density: P(t)
Dissipation Density: D(t)

(b) $T = 5.0$

Bibliography

[1] M. P. Magiera, L. Brendel, D. E. Wolf, and U. Nowak. Spin excitations in a monolayer scanned by a magnetic tip. *EPL (Europhysics Lett.*, 87(2):26002, 2009.

[2] Martin P. Magiera, Sebastian Angst, Alfred Hucht, and Dietrich E. Wolf. Magnetic friction: From Stokes to Coulomb behavior. *Phys. Rev. B*, 84(21):212301, dec 2011.

[3] Martin P. Magiera, L. Brendel, D. E. Wolf, and U. Nowak. Spin waves cause non-linear friction. *Europhys. Lett.*, 95:17010, 2011.

[4] Roy J. Glauber. Time-Dependent Statistics of the Ising Model. *J. Math. Phys.*, 4(2):294, 1963.